SCIENCE CHINA
Technological Sciences

• Article •

December 2014 Vol.57 No.12: 2542–2550
doi: 10.1007/s11431-014-5690-2

A hybrid dynamic programming-rule based algorithm for real-time energy optimization of plug-in hybrid electric bus

ZHANG YaHui[1,2], JIAO XiaoHong[1], LI Liang[2*], YANG Chao[1,2], ZHANG LiPeng[2] & SONG Jian[2]

[1] *Institute of Electric Engineering, Yanshan University, Qinhuangdao 066004, China;*
[2] *State Key Laboratory of Automotive Safety and Energy, Tsinghua University, Beijing 100084, China*

Received May 24, 2014; accepted September 5, 2014; published online October 28, 2014

The optimization of the control strategy of a plug-in hybrid electric bus (PHEB) for the repeatedly driven bus route is a key technique to improve the fuel economy. The widely used rule-based (RB) control strategy is lacking in the global optimization property, while the global optimization algorithms have an unacceptable computation complexity for real-time application. Therefore, a novel hybrid dynamic programming-rule based (DPRB) algorithm is brought forward to solve the global energy optimization problem in a real-time controller of PHEB. Firstly, a control grid is built up for a given typical city bus route, according to the station locations and discrete levels of battery state of charge (*SOC*). Moreover, the decision variables for the energy optimization at each point of the control grid might be deduced from an off-line dynamic programming (DP) with the historical running information of the driving cycle. Meanwhile, the genetic algorithm (GA) is adopted to replace the quantization process of DP permissible control set to reduce the computation burden. Secondly, with the optimized decision variables as control parameters according to the position and battery *SOC* of a PHEB, a RB control is used as an implementable controller for the energy management. Simulation results demonstrate that the proposed DPRB might distribute electric energy more reasonably throughout the bus route, compared with the optimized RB. The proposed hybrid algorithm might give a practicable solution, which is a tradeoff between the applicability of RB and the global optimization property of DP.

plug-in hybrid electric bus (PHEB), control strategy optimization, dynamic programming (DP), genetic algorithm (GA), city bus route

Citation: Zhang Y H, Jiao X H, Li L, et al. A hybrid dynamic programming-rule based algorithm for real-time energy optimization of plug-in hybrid electric bus. Sci China Tech Sci, 2014, 57: 2542–2550, doi: 10.1007/s11431-014-5690-2

1 Introduction

Recently, the plug-in hybrid electric bus (PHEB) became widely applied in the public transportation field in China, because it might achieve a better overall fuel economy than the conventional hybrid electric vehicle (HEV) by partly utilizing the cheaper electric grid energy [1]. The fuel economy of a PHEB depends on its control strategy, which might coordinate the distribution of the power demand between the engine and the electric motor (EM) [2,3]. Thus, the optimal control strategy for the repeatedly driving route is critical to minimize the fuel consumption of the PHEB without impairing the drivability [4].

Several static optimization algorithms, such as differential evolution algorithm [5] and genetic algorithm (GA) [6], have been applied in the optimization of control parameters of the rule-based (RB) strategy, which is easy to realize in engineering. A representative hybrid GA was brought forward to optimize the threshold parameters of a charge depleting-

*Corresponding author (email: liangl@tsinghua.edu.cn)

charge sustaining (CDCS) control strategy, which is a frequently used RB algorithm in the PHEB [7]. However, the optimized RB algorithm is lacking in global optimization property [8]. To overcome this disadvantage, many optimization-based strategies have been proposed [2,9]. Of which one is commonly referred to as dynamic programming (DP), which is a global optimization algorithm. A DP could compute the optimal distribution of the power between the engine and the EM, according to a given driving cycle. However, DP requires knowledge of the entire driving cycle in advance and it has an unacceptable computation complexity for the real-time application [2].

In this paper, a novel hybrid dynamic programming-rule based (DPRB) algorithm is brought forward to solve the global energy optimization problem in real-time microcontroller of a PHEB. Firstly, a control point grid is built for a typical city bus route, according to the station locations and the discrete levels of battery state of charge (*SOC*). The decision variables for the energy optimization at any possible points of the control grid could be deduced with an off-line DP with historical running information of the driving cycle. In order to reduce the computation burden, the genetic algorithm (GA) is adopted to replace the quantization process of DP permissible control set. After that, a RB control, which uses the optimized decision variables on each point of the control grid as control parameters according to the operation states of a PHEB, such as the vehicle position and the battery *SOC*, is adopted as an implementable control method for the energy management. This proposed DPRB might provide a solution, which is a tradeoff between the applicability of RB and the global optimization property of DP.

A backward model for PHEB is built in Section 2. The DPRB and its scheme are proposed in Section 3. The simulation validation over DPRB and CDCS is given in Section 4. Finally, Section 5 gives the conclusion and discussion.

2 Model of electromechanical coupling system

The PHEB structure is a typical single-axle parallel configuration which is sketched in Figure 1. Compared with the conventional vehicle with automatic mechanical transmission (AMT), a disc type EM is joined coaxially between the automatic clutch and AMT. A Hengtong CKZ6116PHEV quick-charge plug-in gas/electric hybrid bus is treated as the prototype. The basic parameters of the prototype are shown in Table 1.

A backward simulation model of PHEB is built [2,8]. According to the vehicle longitudinal dynamics equation, the torque of wheel can be expressed as follows:

$$\begin{aligned} T_w &= \eta_T i_g i_f (T_e + T_m) + T_b \\ &= \left(mgf_r \cos\theta + \frac{1}{2} C_D \rho_d A V^2 + mg \sin\theta + \delta m \frac{\mathrm{d}V}{\mathrm{d}t} \right) r, \end{aligned} \quad (1)$$

where T_w is the torque of wheel, η_T is the transmission efficiency, i_g and i_f represent the gear ratio of AMT and the final drive ratio, respectively. T_e and T_m are the engine torque and the EM torque, respectively. T_b is the braking torque acting on the wheel. m represents the total mass which is the sum of the vehicle mass m_v and passenger mass m_p. The other parameters are shown in Table 2.

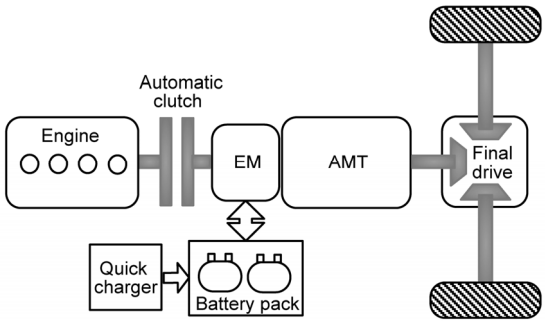

Figure 1 Single-axle parallel configuration of the PHEB structure.

Table 1 Basic parameters of the prototype

Component	Description
Engine	YC6G230N, CNG, 6.454 L, nominal power: 170 kW
EM	Permanent magnet, max torque: 750 Nm nominal power: 94 kW, peak power: 121 kW
Battery	Lithium titanate, capacity: 60 Ah, nominal voltage: 346 V
Gearbox	6-speed AMT, gear ratios: 6.39/3.97/2.4/1.48/1/0.73
Final drive	5.571

The compressed natural gas (CNG) consumption rate Q_g (mL/s) of a CNG engine can be described as follows:

$$Q_g = \frac{P_e b}{367.1 \rho_g g}, \quad (2)$$

where P_e is the engine power calculated through the equation: $P_e = T_e \omega_e$. b is the compressed natural gas consumption rate corresponding to the current engine torque and rotational

Table 2 Parameters of the PHEB model

Parameter	Value
Vehicle mass m_v (kg)	12500
Gravity acceleration g (m/s^2)	9.8
Vehicle speed V (m/s)	–
Rolling resistance coefficient f_r	f_r=0.0076+0.0002016V
Road slope angle θ (rad)	–
Air drag coefficient C_D	0.51
air density ρ_d (kg/m^3)	1.2258
Frontal area A (m^2)	8.25
Wheel radius r (m)	0.48
Correction coefficient of rotating mass δ	1.1

speed, which can be obtained through the calibration test. ρ_g represents the density of CNG.

The EM power P_{EM} can be calculated as follows:

$$P_{EM}=\begin{cases}T_m\omega_m/\eta_{EM}, & \text{motor},\\ T_m\omega_m\eta_{EM}, & \text{generator},\end{cases} \tag{3}$$

where η_{EM} is the EM efficiency.

Based on a basic physical model of battery, the dynamics of battery *SOC*, internal current *I*, and battery power P_{ess} (W) can be expressed as follows:

$$\frac{\mathrm{d}SOC}{\mathrm{d}t}=-\frac{V_{oc}-\sqrt{V_{oc}^{\ 2}-4R_{int}P_{EM}}}{2R_{int}Q_B}, \tag{4}$$

$$I=-\frac{\mathrm{d}SOC}{\mathrm{d}t}Q_B, \tag{5}$$

$$P_{ess}=V_{oc}I, \tag{6}$$

where V_{oc}, R_{int}, and Q_B are the open-circuit voltage, internal resistance, and the capacity of battery, respectively.

3 Scheme of DPRB

The whole diagram of the DPRB scheme which includes a real-time controller and an off-line DP, is shown in Figure 2. In Part I, a RB control strategy whose control parameters are selected according to the position and battery *SOC* of a PHEB is used as an implementable real-time controller. For example, the RB control parameters of PHEB running on the section between station st_n and station st_{n+1} are selected as $\boldsymbol{Rule}^n$, which is determined by the *SOC* S^n at station st_n. In Part II, a control grid is built for a typical city bus route according to the station locations and discrete *SOC* levels, and an off-line DP with historical running information of the driving cycle is used to deduce optimal control parameters of RB on all points of the control grid. However, in order to reduce the computation burden, GA is adopted to replace the quantization process of DP permissible control set. Meanwhile, historical running information, prices of electricity and CNG all might influence the optimal result of DP, i.e. the optimal control grid. So if one of the above factors changes dramatically, the optimal control grid should be recomputed to update the control grid of real-time controller.

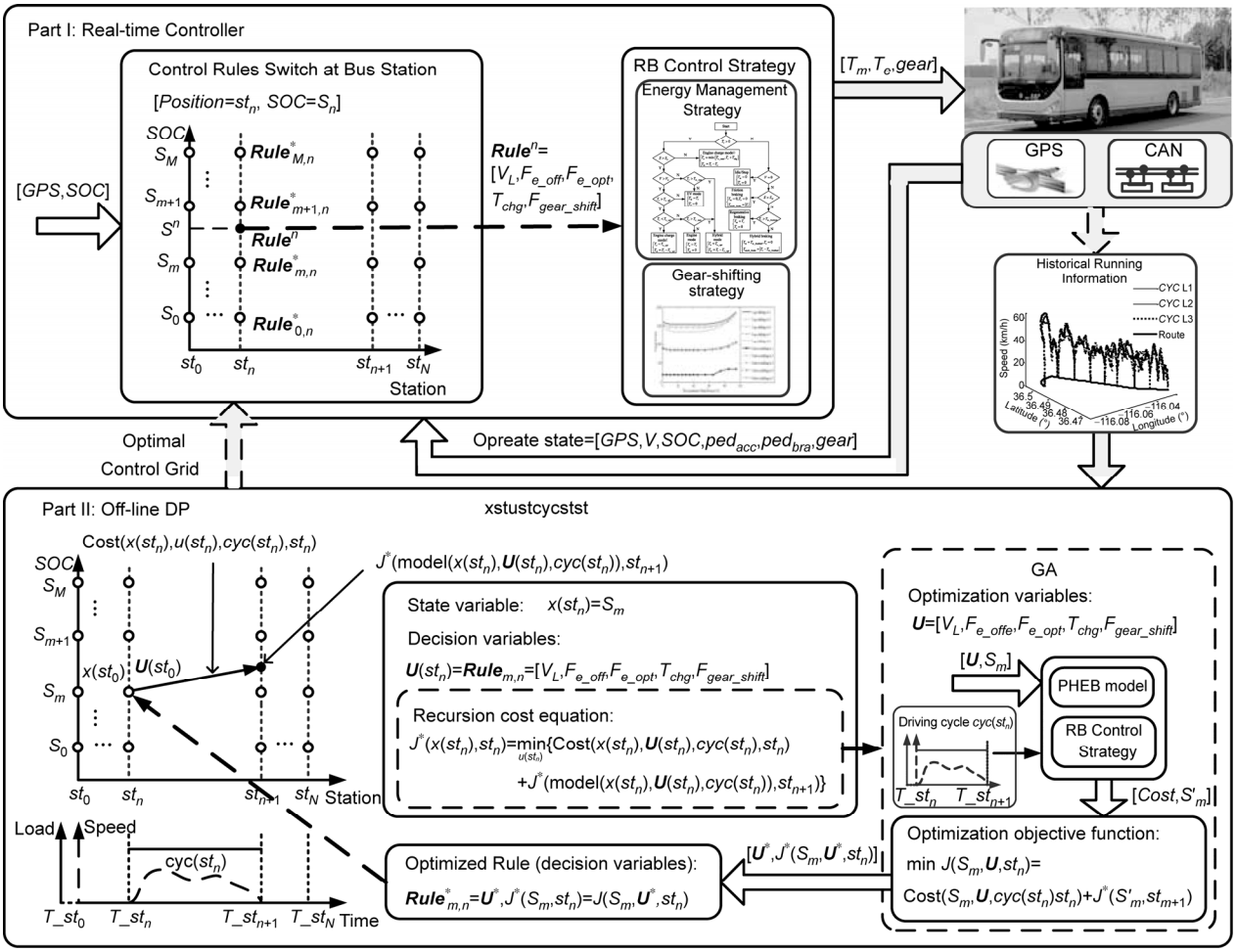

Figure 2 Schematic diagram of DPRB.

3.1 RB control strategy

3.1.1 Statement of RB control parameters

The control parameters of a typical RB adopted in PHEB might be defined as follows [5,6]:

$$\boldsymbol{Rule} = [S_H, S_L, V_L, F_{e\_off}, F_{e\_opt}, T_{chg}, F_{gear\_shift}], \tag{7}$$

where S_H, S_L, V_L, F_{e_off}, F_{e_opt} and T_{chg} represent the higher bound of *SOC*, the lower bound of *SOC*, the vehicle speed below which vehicle operates as a zero emissions vehicle, the factor of engine off-torque envelope, the engine charging torque, and the factor of engine optimal torque envelope, respectively. F_{gear_shift} is a factor which is used to express the control parameters of AMT gear-shifting strategy.

3.1.2 Energy management strategy

The flow chart of RB energy management strategy in the PHEB is shown in Figure 3. *S* is the current value of *SOC*. T_r, T_e, T_m, T_{mech_brake}, and $T_{m\_bralimit}$ represent the driver's require torque, the engine torque, the EM torque, the friction braking torque, and the upper bound of EM regenerative braking torque, respectively. $T_{e\_\max}$, T_{e_off} and T_{e_opt} are the engine max-torque, the engine off-torque, and the engine optimal torque, respectively [5]. T_{e_off} and T_{e_opt} can be expressed as follows:

$$T_{e\_off} = F_{e\_off} T_{e\_\max}, \tag{8}$$

$$T_{e\_opt} = F_{e\_opt} T_{e\_\max}. \tag{9}$$

3.1.3 RB gear-shifting strategy of AMT

A double-parameter RB shifting strategy for 6-speed AMT is adopted for the PHEB [10]. The curves of AMT gear-shifting strategy are the key parameters, which significantly affect the fuel economy and dynamic performances of the PHEB [1]. To achieve an appropriate group of gear-shifting curves, a factor of the gear-shifting curve is proposed, and the appropriate group of gear-shifting curves can be expressed as follows:

$$f_{opt}(\alpha, V) = F_{gear\_shift} f_{ref}(\alpha, V), \tag{10}$$

where $f_{ref}(\alpha,V)$,α, and V represent the factor, the group of reference gear-shifting curves, the acceleration pedal position, and the vehicle speed, respectively.

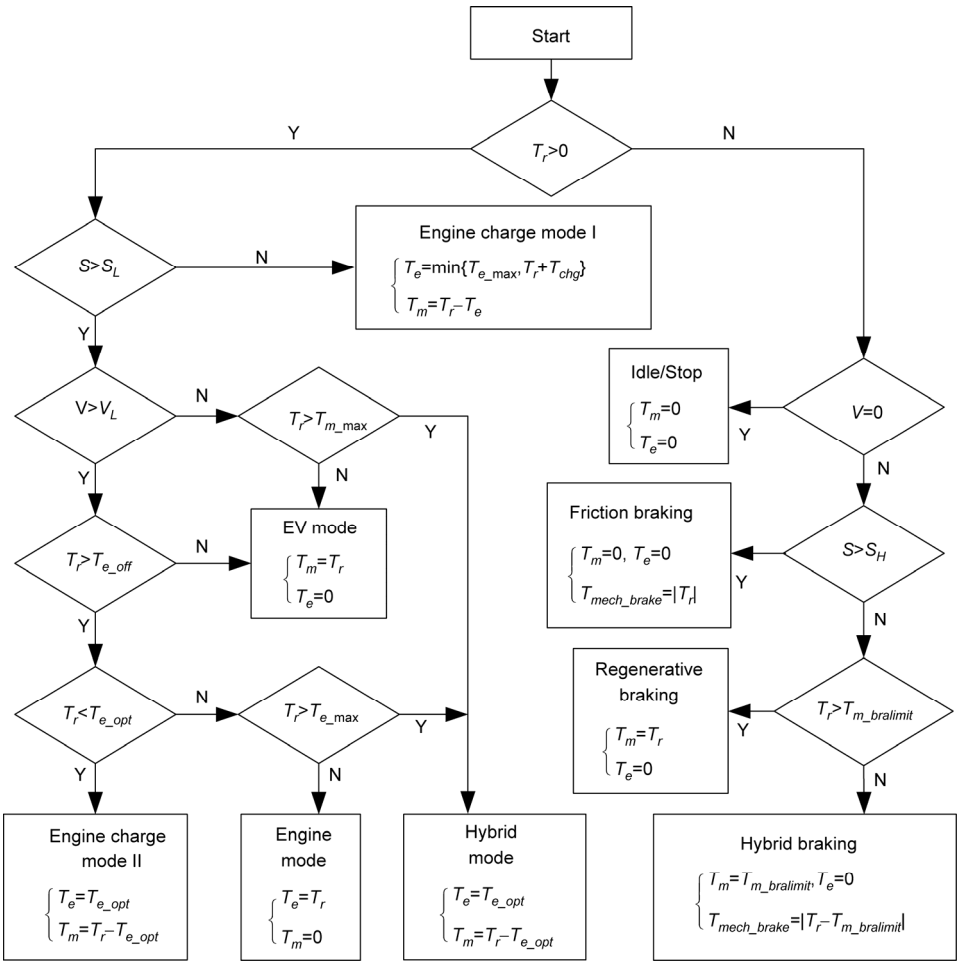

Figure 3 Flow chart of the RB energy management strategy.

3.2 Optimization of key control parameters in DPRB

3.2.1 Statement of optimization problem

A bus route might be divided into N sections according to its station locations, as shown in Figure 2. The state variable at each divided key point might be defined as follows [2]:

$$x(st_n) = SOC(st_n), \tag{11}$$

where $SOC(st_n)$ is the battery SOC at station st_n. $SOC(st_0)$ is the given initial SOC and $SOC(st_N)$ is the unrestraint final SOC at the terminal station. The state variable satisfies the following constraint:

$$S_L \leqslant SOC(st_n) \leqslant S_H. \tag{12}$$

The preparative decision variables are the same as defined in the RB algorithm as eq. (10) describes. Considering the specifications of lithium titanate battery, as illustrated in Figure 4, the charged resistance R_{chg} and discharged resistance R_{dis} of a battery cell are obviously increased when the battery is over charged or over discharged, which might result in unpredictable and shortened battery life [11]. Thus, the control parameters S_H and S_L might be experientially defined as 0.9 and 0.3. Then the dimension of decision variables is reduced as follows:

$$\boldsymbol{u}(st_n) = \left[V_L(st_n), F_{e\_off}(st_n), F_{e\_opt}(st_n), F_{gear\_shift}(st_n)\right], \tag{13}$$

where the decision variables $\boldsymbol{u}(st_n)$ are bounded by Table 3 according to the configuration parameters of the given PHEB.

The optimization of $\boldsymbol{u}(st_n)$ for the repeatedly driven bus route might be described as follows [9].

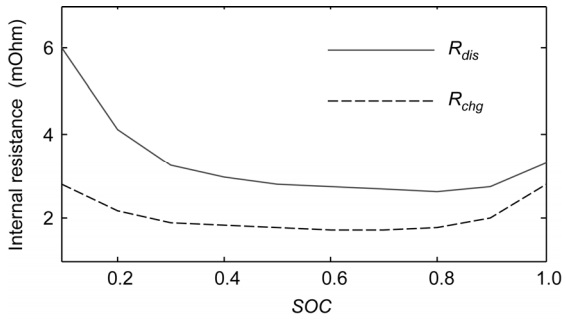

Figure 4 Discharged resistance and charged resistance of a cell (At 6 C charge rates on 45°C).

Table 3 Range of the decision variables

Decision variable	Unit	Lower bound	Higher bound
V_L	km/h	0	30
F_{e_off}	–	0.2	0.4
F_{e_opt}	–	0.4	0.7
T_{chg}	Nm	50	150
F_{gear_shift}	–	0.9	1.1

Firstly, a permissible decision sequence $\{\boldsymbol{u}(st_0), \boldsymbol{u}(st_1),\cdots, \boldsymbol{u}(st_{N-1})\}$ is found to minimize the objective function J, when the system transfers from the initial state $x(st_0)$ at the initial station to the final state $x(st_N)$ at the terminal station st_N. J is the integral energy consumption cost function (unit: yuan (RMB)):

$$J = \sum_{n=0}^{N-1} \mathrm{Cost}\left(x(st_n), \boldsymbol{u}(st_n), cyc(st_n), st_n\right), \tag{14}$$

where $\mathrm{Cost}\left(x(st_n), \boldsymbol{u}(st_n), cyc(st_n), st_n\right)$ represents the energy consumption cost of PHEB running on the section between station st_n and station st_{n+1}, and it is determined by the decision variables $\boldsymbol{u}(st_n)$ and the driving cycle $cyc(st_n)$ in this section.

Then, the system state transition equation might be expressed as follows:

$$\begin{aligned} x(st_{n+1}) &= \mathrm{model}\left(x(st_n), \boldsymbol{u}(st_n), cyc(st_n)\right) \\ &= x(st_n) + \int_{T\_st_n}^{T\_st_{n+1}} -I/Q_g \,\mathrm{d}t,\ n = 0,1,\cdots,N-1, \end{aligned} \tag{15}$$

where $\mathrm{model}(\cdot)$ is the system state transition function, and it is a vehicle model which can be used to calculate the energy consumption of PHEB. T_st_n and T_st_{n+1} are the start and stop time of the driving cycle on the section between station st_n and station st_{n+1}.

3.2.2 Optimization algorithm

According to Bellman's Principle of Optimality [12], the recursion cost equation to calculate the minimum energy consumption cost function might be expressed as follows:

$$\begin{aligned} J^*\left(x(st_n), st_n\right) = \min_{\boldsymbol{u}(st_n)} \Big\{ &\mathrm{Cost}\left(x(st_n), \boldsymbol{u}(st_n), cyc(st_n), st_n\right) \\ &+ J^*\left(\mathrm{model}\left(x(st_n), \boldsymbol{u}(st_n), cyc(st_n)\right), st_{n+1}\right)\Big\}, \\ n = N-1, N-2, \cdots, 1, 0, \end{aligned} \tag{16}$$

$$J^*\left(x(st_N), st_N\right) = 0, \tag{17}$$

where $J^*(x(st_n), st_n)$ represents the minimum energy consumption cost during the process which starts from any state $x(st_n)$ at the nth phase until the process is finished.

The optimization algorithm consists of two procedures: backwards and forwards [12,13]. Firstly, the recursive cost equation is solved backwards to search for the optimal cost $J^*(x(m,st_n),st_n)$ and the corresponding optimal decision variables $\boldsymbol{u}(x(m, st_n), st_n)$ for every state $x(m, st_n)$. Secondly, it is computed forwards by the state transition eq. (12) to restore the optimal state trajectory and the optimal decision sequence:

$$\boldsymbol{\pi}^* = \left\{\boldsymbol{u}^*(st_0), \boldsymbol{u}^*(st_1), \cdots, \boldsymbol{u}^*(st_{N-1})\right\}. \tag{18}$$

The above computation procedures might be usually solved by numerical method using quantization and interpolation [12]. Quantization is the discretization of accessible state set and permissible control set. The cost function $J(x(m,st_n),st_n)$ is calculated only at the points of control grid. However, there is no guarantee that the next state variable $x(st_{n+1})$ could be a quantized value. So the value of optimal cost function $J^*(\text{model}(x(st_n), \boldsymbol{u}(st_n), cyc(st_n)), st_{n+1})$ is determined by the interpolation. In addition, the optimal decision sequence restored forwards is also determined by the interpolation.

In order to restrain the interpolation errors, the quantization precision should be improved [2]. Then the computation complexity might be obviously increased, especially for the problem with high-dimensional decision variable. To alleviate this problem, GA [14] is employed in the optimization algorithm to replace the quantization process of permissible control set to optimize the proposed five-dimensional decision variables. Therefore, the optimization variables in GA is defined as eq. (13), that is as follows:

$$\boldsymbol{u} = \left[V_L, F_{e\_off}, F_{e\_opt}, T_{chg}, F_{gear\_shift}\right]. \tag{19}$$

Therefore, on a certain point of the control grid, the optimization objective function in GA can be defined as

$$J\left(S_m, \boldsymbol{u}, st_n\right) = \text{Cost}\left(S_m, \boldsymbol{u}, cyc(st_n), st_n\right) + J^*\left(S'_m, st_{n+1}\right), \quad n = N-1, \cdots, 1, 0,\ m = 0, 1, \cdots, M, \tag{20}$$

$$S'_m = \text{model}\left(S_m, \boldsymbol{u}, cyc(st_n)\right), \tag{21}$$

subjected to

$$\begin{cases} i_{\max}(\boldsymbol{u}) \geqslant 20\%, \\ t_{\min}(\boldsymbol{u}) \leqslant 25 \text{ s}, \\ a_{\max}(\boldsymbol{u}) \geqslant 0.1 \text{ g}, \end{cases} \tag{22}$$

where $i_{\max}$, $t_{\min}$ and $a_{\max}$ are the grade-ability with half load at 10 km/h, the acceleration time for 0–50 km/h and the maximum acceleration. $J^*(S'_m, st_{n+1})$ is obtained by using linear interpolation among the optimal cost on the points of control grid at section st_{n+1}. $\text{Cost}(S_m, \boldsymbol{u}, cyc(st_n), st_n)$ represents the energy consumption cost of PHEB which runs on the section between station st_n and station st_{n+1}, adopting a group of control parameters $\boldsymbol{u}$ and a given initial state S_m. The cost might be expressed as follows:

$$\begin{aligned} &\text{Cost}\left(S_m, \boldsymbol{u}, cyc(st_n), st_n\right) \\ &= p_f \int_{T\_st_n}^{T\_st_{n+1}} \frac{1}{10^6} Q_g \mathrm{d}t + \frac{p_e}{\eta_{elec}} \int_{T\_st_n}^{T\_st_{n+1}} \frac{1}{3.6\times10^6} P_{ess} \mathrm{d}t \\ &= \frac{p_f}{10^6} \int_{T\_st_n}^{T\_st_{n+1}} \frac{T_e \omega_e b}{367.1 \rho_g g} \mathrm{d}t + \frac{p_e}{3.6\times10^6 \eta_{elec}} \int_{T\_st_n}^{T\_st_{n+1}} V_{oc} I \mathrm{d}t, \end{aligned} \tag{23}$$

where p_f and p_e are the market price of CNG and electricity. η_{elec} is the efficiency of the power grid to charge the battery.

The fitness function of GA is based on a simple linear scheduling method [15], and the constraints described by eq. (22) are implemented using penalty functions that indicate the inferior solutions by decreasing their fitness values. Here, the fitness function is finally defined as

$$\text{fit}(\boldsymbol{u}) = 2 - 2\times\frac{Pos-1}{Nind-1} + \sum_{i=1}^{3} \alpha_i P_i(\boldsymbol{u}), \tag{24}$$

where *Nind* is the population size, *Pos* is the individual's numerical order in the sequence which is sorted in ascending order according to the objective function value $J(S_m, \boldsymbol{u}, st_n)$ of individual in current population. $P_i(\boldsymbol{u})$ is the penalty function corresponding to the ith constraint and α_i is the penalty factor.

4 Simulation

4.1 Simulation conditions

A typical city driving cycle *CYC* is developed based on the 14-round trips traffic records, including the speed-time sequences and the changes of passenger number, collected from the city bus route which has a one-way distance of 7.3 km and 9 stations containing the initial station. The raw speed-position sequences of three actual round trips *CYC*1, *CYC*2 and *CYC*3 are shown in Figures 5 and 6. The speed-time sequence and passenger-position sequence of *CYC* are shown in Figures 7 and 8, respectively. The driving cycle is divided into 16 phases according to bus stations and the discrete sequence of battery *SOC* is defined as [0.3, 0.4, 0.5, 0.6, 0.7, 0.8, 0.9]. Then a control grid is constructed with N=16 and M=7.

A unified initial population is generated using the orthogonal design method [16], and applied to the optimization of

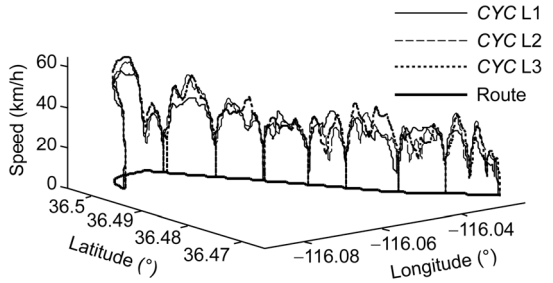

Figure 5 Speed-position sequences of the three leave trips.

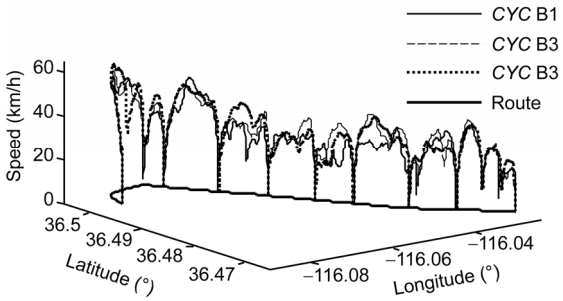

Figure 6 Speed-position sequences of the three return trips.

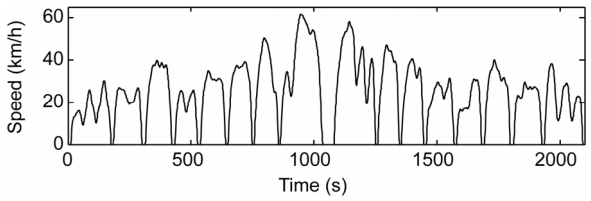

Figure 7 Speed-time sequences of *CYC*.

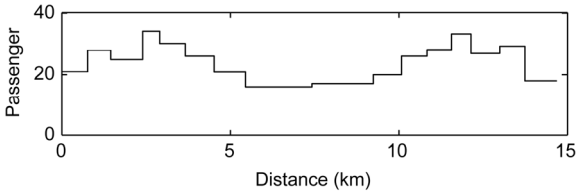

Figure 8 Passenger-distance sequences of *CYC*.

control parameters at each point of the control grid. $L_{25}(5^6)$, which is an orthogonal array for 5 factors and 6 levels, is applied to select 25 representative combinations to generate the unified initial population.

The penalty function in eq. (24) is defined as follows:

$$P_i(\boldsymbol{u}) = \begin{cases} 0, & \text{the } i\text{th constraint is satisfied,} \\ 1, & \text{otherwise.} \end{cases} \tag{25}$$

The other relevant parameters are listed in Table 4.

4.2 Simulation results

In the simulation, DPRB and the widely used CDCS optimized by GA, have been implemented on *CYC* and the three actual round trips *CYC*1, *CYC*2 and *CYC*3, respectively. In order to analyze the results of DPRB when the initial *SOC* value is changed, simulations then have been conducted on a series initial *SOC* values: 0.8, 0.7 and 0.6.

The results of the two control methods over the driving cycle *CYC* with the initial battery *SOC* 0.9 are shown in Figure 9, including the histories of *SOC*, engine torque, EM torque and gear number during the driving cycle. The operating points of engine and EM are shown in Figure 10, in

Table 4 The other relevant parameters

Parameter	Value
Market price of CNG p_f (yuan/m^3)	4.6
Market price of electricity p_e (yuan/kWh)	1
The 1st penalty factor α_1	–0.5
The 2nd penalty factor α_2	–0.5
The 3rd penalty factor α_3	–0.5
Average mass of passenger $\overline{m}_p$ (kg)	60
Population size *Nind*	25
Maximum generation number *Men*	30
Efficiency of power grid charge battery η_{elec}	0.9

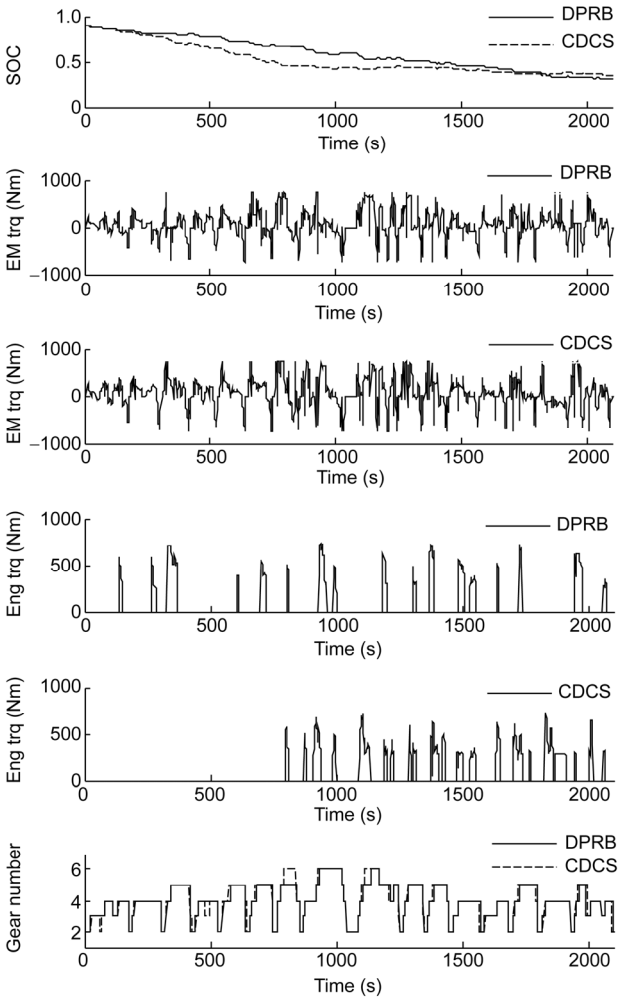

Figure 9 Results of DPRB and CDCS during *CYC*.

which (a) and (b) are the operating points of engine and EM of CDCS, meanwhile (c) and (d) are those of the optimized DPRB. From the comparation, DPRB makes the depletion of *SOC* more reasonable during the driving cycle and operates the engine at a higher efficiency working area.

The above performances are insensitive to the initial *SOC* values, and they might be flexibly ensured through selecting the optimized control parameters at the corresponding point of the control grid. As for this point, the evidence is shown in Figure 11, there are histories of *SOC* of DPRB and CDCS during the driving cycle *CYC* based on three initial *SOC* values of 0.8, 0.7 and 0.6.

In addition, in the quantization process of DP permissible control set on a certain point of the control grid, supposing that each decision variable is quantified in six levels, then the number of algorithm computation cycles might be 6^5=7776. While with the proposed algorithm, the number is reduced to 657 with the population size and maximum generation number of GA is selected as 25 and 30, respectively.

The energy consumption costs, which are composed of the CNG consumption costs and the electricity consumption

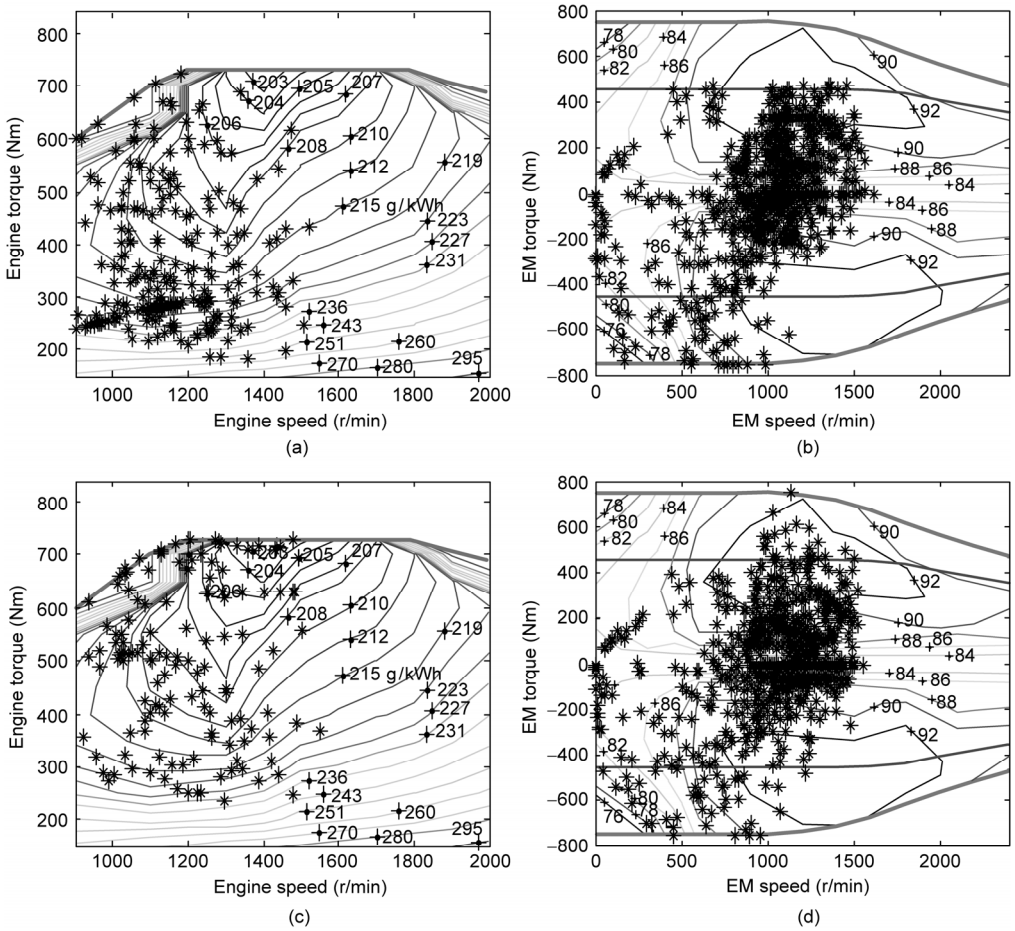

Figure 10 Operating points of engine and EM. (a) Operating points of engine of CDCS; (b) operating points of EM of CDCS; (c) operating points of engine of DPRB; (d) operating points of EM of DPRB.

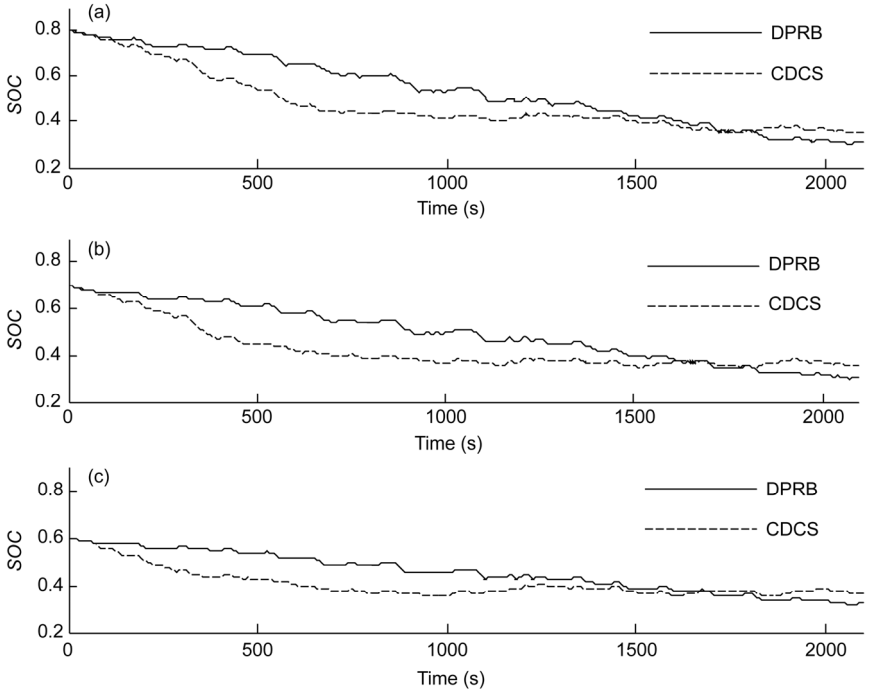

Figure 11 Trends of *SOC* with different initial values. (a) Histories of *SOC* based the initial *SOC* value of 0.8; (b) histories of *SOC* based the initial *SOC* value of 0.7; (c) histories of *SOC* based the initial *SOC* value of 0.6.

costs, based on DPRB and CDCS during driving cycles of *CYC*, *CYC*1, *CYC*2 and *CYC*3 with four initial *SOC* values of 0.9, 0.8, 0.7 and 0.6 are listed in Table 5. The DPRB saves 5.30%~7.87% energy consumption cost, compared with the optimized CDCS, even for the actual driving cycles with randomness and uncertainty.

5 Conclusion and discussion

A novel hybrid DPRB algorithm is brought forward to solve the global energy optimization problem in the real-time controller of PHEB. DPRB makes the depletion of *SOC* reasonable during the driving cycle and operates the engine at a high efficiency working area. Simulation results demonstrate that the DPRB saves 5.30%~7.87% energy consumption cost, compared with the optimized CDCS, even for the actual driving cycles with randomness and uncertainty. In addition, the computation burden is obviously reduced by adopting GA to replace the quantization process of DP permissible control set. In DPRB, RB control is adopted as an implementable control method, and off-line DP with historical running information of the route ensures the global optimization property of DPRB. Therefore, a solution, which is a tradeoff between the applicability of RB and the global optimization property of DP, is given by DPRB.

With the wide application of on-board GPS, it is available for PHEB to look up the control grid according to the bus location and battery *SOC*. The future work is to test the proposed DPRB in a real controller with an actual PHEB.

Table 5 Comparison of energy consumption costs (unit: yuan)

Cycle	Strategy	Initial *SOC* value			
		0.9	0.8	0.7	0.6
CYC	CDCS	14.0401	14.4011	15.1225	15.5920
	DPRB	12.9352	13.5024	14.2018	14.6837
	Saving	7.87%	6.24%	6.09%	5.83%
*CYC*1	CDCS	13.5522	14.2000	14.7214	15.4179
	DPRB	12.5175	13.2318	13.8128	14.5618
	Saving	7.64%	6.82%	6.17%	5.55%
*CYC*2	CDCS	14.5475	15.0665	15.5087	15.9493
	DPRB	13.4788	14.1175	14.5535	15.0162
	Saving	7.35%	6.30%	6.16%	5.85%
*CYC*3	CDCS	14.4034	14.9523	15.3777	15.8835
	DPRB	13.3800	13.9171	14.4428	15.0410
	Saving	7.10%	6.92%	6.08%	5.30%

This work was supported by the National Natural Science Foundation of China (Grant No. 51275557, 5142505), and the National Science-Technology Support Plan Projects of China (Grant No. 2013BAG14B01).

1 Yang C, Jiao X H, Li L, et al. Electromechanical coupling driving control for single-shaft parallel hybrid powertrain. Sci China Tech Sci, 2014, 57: 1–9
2 Gong Q M, Li Y Y, Peng Z R. Trip-based Optimal Power Management of Plug-in Hybrid Electric Vehicles. IEEE Trans Veh Tech, 2012, 57: 3393–3401
3 Sun D Y, Lin X Y, Qin D T, et al. Power-balancing instantaneous optimization energy management for a novel series-parallel hybrid electric bus. Chin J Mech E, 2012, 25: 1161–1170
4 Desai C. Design and optimization of hybrid electric vehicle drivetrain and control strategy parameters using evolutionary algorithms. Dissertation of Masteral Degree. Canada: Concordia University, 2010. 10–16
5 Wu L H, Wang Y N, et al. Multi-objective optimization of HEV fuel economy and emissions using the self-adaptive differential evolution algorithm. IEEE T Veh Technol, 2011, 60: 2458–2470
6 Montazeri-Gh M, Poursamad A, Ghalichi B. Application of genetic algorithm for optimization of control strategy in parallel hybrid electric vehicles. J Franklin Institute, 2006, 343: 420–435
7 Wirasingha S G, Emadi A. Classification and review of control strategies for plug-in hybrid electric vehicles. IEEE T Veh Technol, 2011, 60: 111–122
8 Torres J L, Gonzalez R, Gimenez A, et al. Energy management strategy for plug-in hybrid electric vehicles. A comparative study. Appl Energ, 2014, 113: 816–824
9 Lin C C, Peng H, Grizzle J W, et al. Power management strategy for a parallel hybrid electric truck. IEEE T Con Sys Tech, 2003, 11: 839–849
10 Wang Y H, Song J, Li X K. Simulation of AMT Autoshift Process Based on Matlab/Simulink/Stateflow. In: SAE 2004 Automotive Dynamics, Stability and Controls Conference. 2004-01-2055
11 Marano V, Onori S, Guezennec Y, et al. Lithium-ion batteries life estimation for plug-in hybrid electric vehicles. In: Proceedings of the IEEE Vehicle Power and Propulsion Conference. Dearborn, 2009. 536–543
12 Rein L. Iterative dynamic programming. Boca Raton: Chapman & Hall/ CRC, 2000
13 Xu W, Peng Y, Wang B D. Evaluation of optimization operation models for cascaded hydropower reservoirs to utilize medium range forecasting inflow. Sci China Tech Sci, 2013, 56: 2540–2552
14 Zhao W Z, WANG C Y. Mixed H_2/H_∞ road feel control of EPS based on genetic algorithm. Sci China Tech Sci, 2012, 55: 72–80
15 Sadjadi F A. Comparison of fitness scaling functions in genetic algorithms with applications to optical processing. Proc SPIE, 2004, 5557: 356–364
16 Leung Y W, Wang Y P. An orthogonal genetic algorithm with quantization for global numerical optimization. IEEE T Evolut Comput, 2001, 5: 41–53